Supporting Information

Manganese-Phosphomolybdate Molecular Catalyst for Electron Transfer Reaction of Ferricyanide to Ferrocyanide

Kaining Gong, Yunping Liu, and Zhangang Han*

[a] College of Chemistry and Material Science, Hebei Normal University, Shijiazhuang, 050024, China. E-mail: hanzg116@126.com

Table S1 Crystal data and structure refinement details for the hybrids **1-3**.

hybrid	**1**	**2**	**3**
Empirical formula	$C_{143}H_{264}Mn_4Mo_{48}N_{22}Na_6O_{262}P_{32}$	$C_{26}H_{62}Mn_2Mo_{12}N_4Na_4O_{71}P_8$	$C_{52}H_{92}Mn_3Mo_{12}N_8Na_3O_{75}P_9$
Formula weight	12436.92	3167.60	3692.96
Crystal system	Monoclinic	Monoclinic	Orthorhombic
Space group	*P2(1)/c*	*C2/c*	*Pnma*
a (Å)	23.0522(11)	21.1291(11)	29.508(19)
b (Å)	15.7570(7)	18.4006(9)	23.454(15)
c (Å)	23.8647(11)	21.8843(11)	15.429(10)
α, *β*, *γ* (°)	90, 90.9170(10), 90	90, 100.7960(10), 90	90, 90, 90
Volume ($Å^3$), *Z*	8667.3(7), 2	8357.8(7), 4	10678(12), 4
Density(calculated)($Mg·m^{-3}$)	2.373	2.509	2.284
Absorption coefficient (mm^{-1})	2.084	2.321	1.961
F(000)	5984	6088	7140
Crystal size (mm^3)	0.21 × 0.19 × 0.15	0.17 × 0.15 × 0.13	0.19 × 0.15 × 0.13
θ (°)	1.77 - 25.01	1.65 - 25.01	1.91 - 25.01
Reflections collected	41517	20341	50207
Independent reflections ($R_{(int)}$)	15263 [$R_{(int)}$ = 0.0288]	7362 [$R_{(int)}$ = 0.0173]	9661 [$R_{(int)}$ = 0.0248]
Max. and min. Transmission	0.732 and 0.652	0.740 and 0.681	0.775 and 0.710
Data/restraints/parameters	15263 / 1308 / 1222	7362 / 43 / 649	9661 / 66 / 766
Goodness-of-fit on F^2	1.067	1.000	1.061
Final *R* indices [$I > 2\sigma(I)$]	R_1 = 0.0472, wR_2 = 0.1193	R_1 = 0.0293, wR_2 = 0.0878	R_1 = 0.0338, wR_2 = 0.1015
R indices (all data)	R_1 = 0.0590, wR_2 = 0.1299	R_1 = 0.0311, wR_2 = 0.0893	R_1 = 0.0373, wR_2 = 0.1050

[a] $R_1 = \sum||F_o| - |F_c|| / \sum|F_o|$; [b] $wR_2 = \sum[w(F^2_o - F^2_c)^2] / \sum[w(F^2_o)^2]^{1/2}$

Table S2. BVS calculations of Mo centers in hybrids **1-3**

	Hybrid **1**	Hybrid **2**	Hybrid **3**
Mo1	5.227	5.193	5.140
Mo2	5.252	5.260	5.158
Mo3	5.207	5.210	5.152
Mo4	5.301	5.228	5.190
Mo5	5.206	5.256	5.166
Mo6	5.233	5.289	5.165

Table S3. BVS calculations of P centers in compounds **1-3**

	Hybrid **1**	Hybrid **2**	Hybrid **3**
P1	4.798	4.801	4.862
P2	4.925	4.862	4.801
P3	4.828	4.803	4.482
P4	4.808	4.851	4.809

Table S4. BVS calculations of Mn centers in compounds **1-3**

	Hybrid **1**	Hybrid **2**	Hybrid **3**
Mn1	1.989	2.157	2.012
Mn2	1.960	1.989	1.962

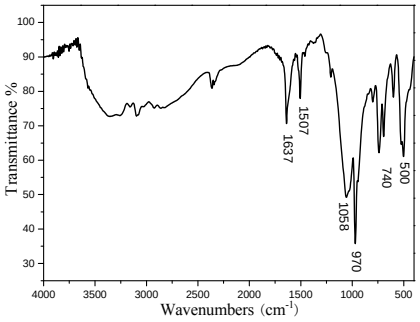

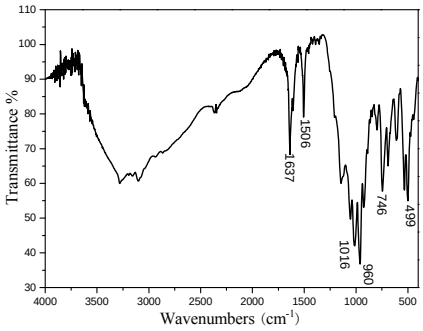

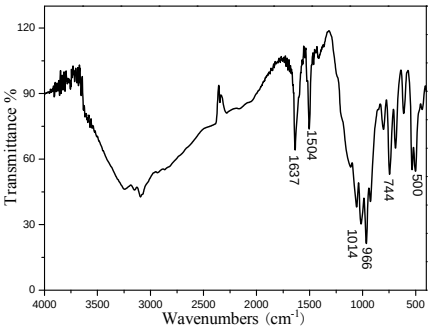

Fig. S1 IR spectra of (a) hybrid **1** (b) hybrid **2** (c) hybrid **3**

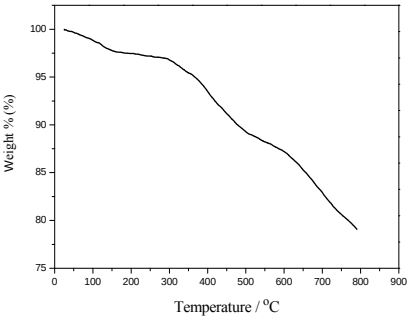

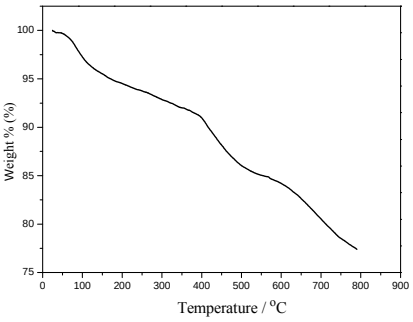

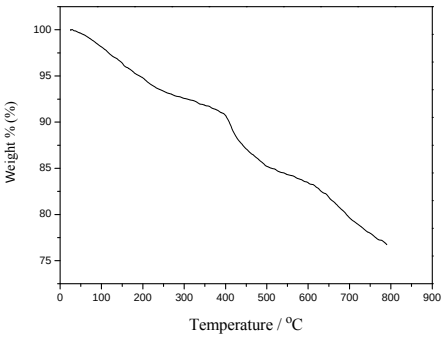

Fig. S2 TG curves of (a) of hybrid **1** (b) TG of hybrid **2** (c) TG of hybrid **3**

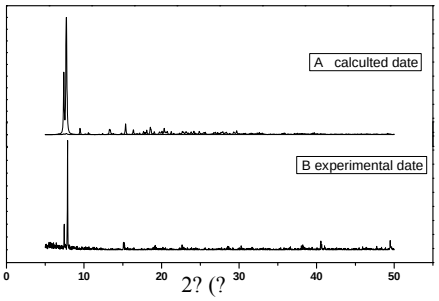

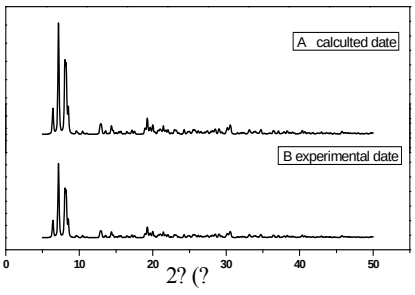

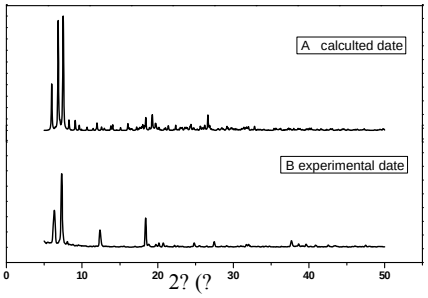

Fig. S3 XRD curves of (a) of hybrid **1** (b) XRD of hybrid **2** (c) XRD of hybrid **3**

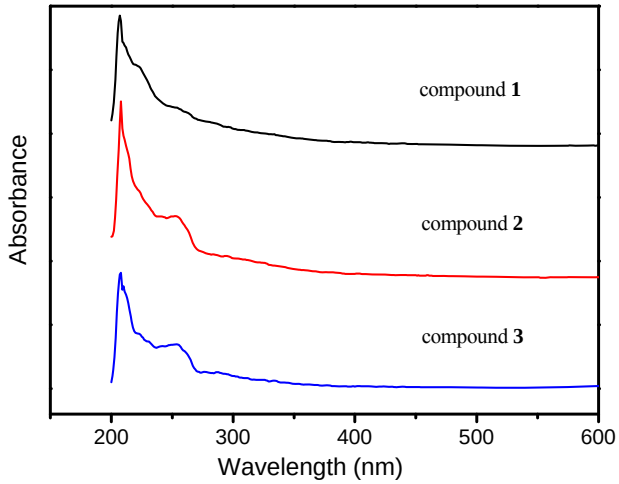

Fig. S4 UV of hybrids **1-3** in methanol

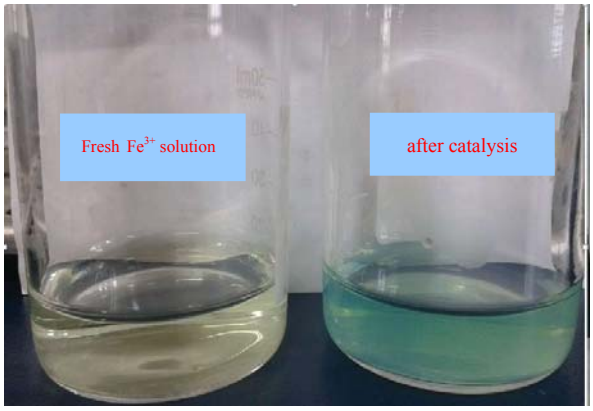

Fig. S5 The colors of solutions of Fe^{3+} to Fe^{2+} with the presence of **1**

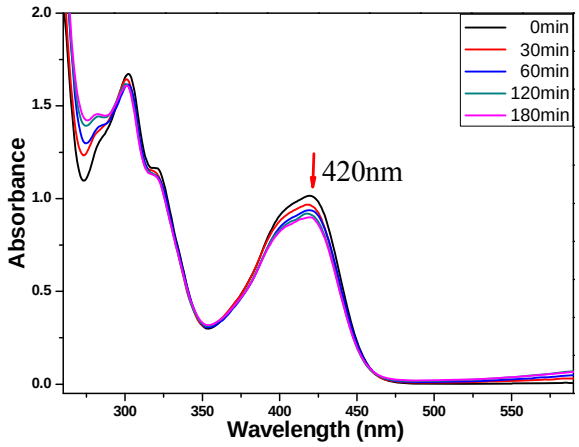

Fig. S6 Successive UV-visible absorption spectra for aqueous solutions of the catalytic reduction reactions of $[Fe(CN)_6]^{3-}$ and $S_2O_3^{2-}$ in the presence of $(H_2bpp)_3[PMo^{VI}_9Mo^{V}_3O_{40}]$

Fig. S7 The solution color of Fe^{3+} with $Na_2S_2O_3$ as reductant with the presence of $H_3PMo_{12}O_{40}$

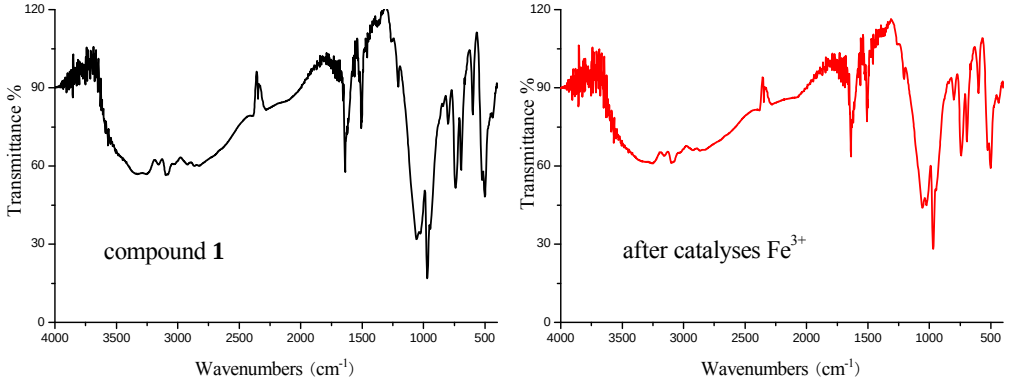

Fig. S8 Comparisons of IR spectra of the hybrid **1**, and after catalysis

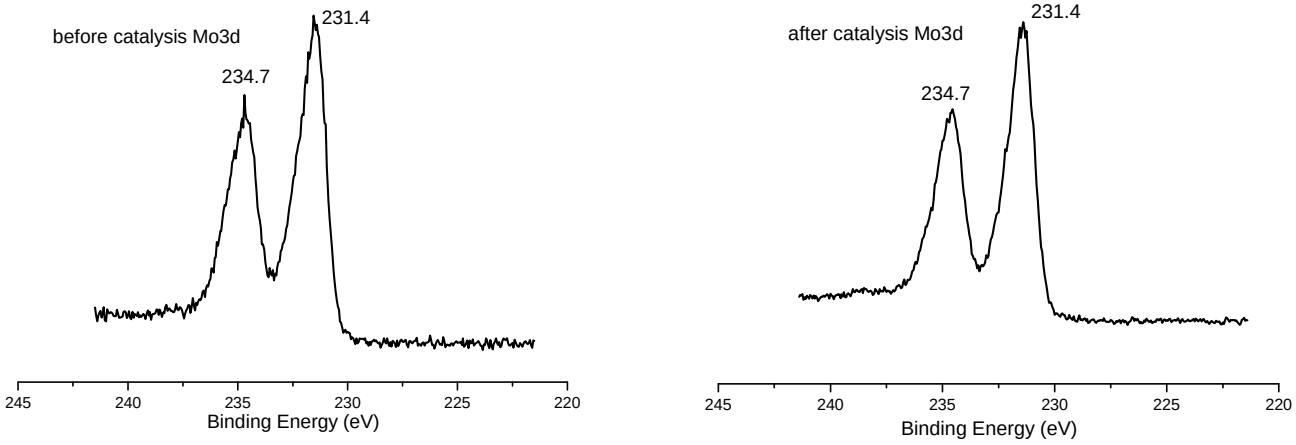

Fig. S9 XPS for Mo of hybrid **1** before catalysis and after catalysis.